A Hierarchical Exploration of Rib Strain in Dynamic Frontal Thoracic Impacts

Akshara Sreedhar, Yun-Seok Kang, John H. Bolte IV, Michelle M. Murach, Jason Stammen, Kevin Moorhouse, Rakshit Ramachandra, Amanda M. Agnew

Abstract Due to high-rate loads placed on the torso during motor vehicle crashes, the human thorax is commonly injured, and resulting rib fractures are linked to fatalities. The goal of this study was to explore the variation in strain modes, magnitudes, and rates of rib levels 3-8 in a dynamic, distributed loading scenario in a series of hierarchical tissue states of 50th percentile males. Strain modes varied by rib level where superior level ribs demonstrated tension on the cutaneous surface, and inferior ribs, rib 8 specifically, experienced compression. Peak strain and peak strain rates varied between rib levels at the anterior and posterior locations ($p<0.0001$). Intact thoraces generally demonstrated higher peak strain values across rib levels and eviscerated thoraces exhibited higher peak strain rates across rib levels. Rib levels 4-6 experienced higher peak strain than other levels at the anterior location while level 8 experienced higher peak strains at the posterior location. After whole thorax testing, ribs 4-7 were removed and tested to failure in anterior-posterior bending. Peak strains from individual rib testing did not vary between rib levels 4-7 at anterior or posterior locations ($p=0.17$ and $p=0.79$, respectively). This study revealed local deformation patterns across ribs while maintaining the structural integrity of the thorax in distributed loading as well as component testing to failure across rib levels. The results from this study can be used to further understand rib connections during loading events and help to define accurate rib-specific properties to improve the biofidelity of computational human body models.

Keywords deformation, rib level, strain modes, tissue states, thorax

I. INTRODUCTION

Despite advances in frontal crash protection, thorax injuries, specifically rib fractures, are still prevalent in occupants of motor vehicle crashes leading to high rates of mortality and morbidity [1-2]. Among different body regions, recent studies reveal that protection of the thorax is still lagging behind other regions [3]. In order to design novel restraint methods to protect the thorax, it is important to further study the thorax in detail to characterize differential response and injury thresholds across all occupants. Previous studies have identified chest deflection as a strong injury predictor in various loading scenarios [4-6]. However, due to complex thoracic anatomy, local deformation patterns need to be better understood in order to improve metrics for identifying injury and injury risk.

In addition to post-mortem human subject (PMHS) tests, finite element (FE) human body models (HBMs) are valuable tools utilized to assess biomechanical response. However, the efficacy of these models in their ability to mimic realistic response and predict injury risks are based on the accuracy of validation data and experimental input data [7-9]. To elucidate the various components of thoracic response, specifically for the purpose of providing comparative data for FE models, sequential thorax tissue state tests were previously conducted [1]. While these test data were useful, localized rib strain behavior in each loading scenario was not provided. Other efforts have been made in studying individual rib response by characterizing geometric, structural, and material properties at the component level across all aspects of the population [9-16]. However, a gap still exists in quantifying how individual rib properties fit into the whole thorax. As an attempt to explore this gap, the effects of structural coupling in denuded and eviscerated thoraces were previously investigated, and superior ribs were found to be more coupled through the sternum to the contralateral rib than inferior ribs [17]. While this is an important finding, the tests were conducted quasi-statically making it difficult to translate these results to dynamic impact scenarios.

A.Sreedhar (sreedhar.6@osu.edu, +1 614 685 2203) is an M.S. student in Mechanical Engineering at The Ohio State University in Columbus, OH, USA. A. Sreedhar, Y.S. Kang, J.H. Bolte IV, M.M. Murach, R. Ramachandra, and A.M. Agnew are affiliated with the Injury Biomechanics Research Center at The Ohio State University, Columbus, OH, USA. J. Stammen and K. Moorhouse are affiliated with the National Highway Traffic Safety Administration, Vehicle Research and Test Center (NHTSA/VRTC) in East Liberty, OH, USA.

Thoraces were investigated in dynamic scenarios in order to characterize the global mechanisms observed in thoracic response by [18]. The effects of thorax geometry and rib rotation at the costovertebral joint were studied and provided interesting insights on non-injurious, localized deformation at each rib level. However, these experiments were conducted by isolating the thorax from the rest of the body prior to conducting anterior-posterior loading. Additionally, the tests were conducted to the bony thorax where contributions of viscera and soft tissue were not evaluated to fully understand the deformation mechanisms. Additional dynamic impacts in side and oblique positions to PMHS have been conducted to explore how loads are transmitted through the thorax in these scenarios [19]. While this study explored small females in addition to 50th males, the focus was on overall thoracic response rather than rib-level deformation. Therefore, there remains a need to better understand individual rib deformation in the context of dynamic anterior-posterior whole thoracic response.

Computed Tomography (CT) imaging has also been utilized to track deformations of ribs while various anterior loads were applied [20]. While this novel method characterized normalized deflection at locations on the ribs, this study was also conducted quasi-statically. Thoracic CT scans have revealed that the rib cage, or the bony thorax, deformed differently than the surrounding skin and musculature [6]. Such imaging techniques are useful to understand general deformation of thoraces based on specific loading scenarios. However, the complexity and rate-dependency of biological tissue warrant further investigation of thoracic response in various conditions. Strain gauges are often used to detect fracture timing in ribs [21] but can also provide insight into local deformation patterns within the thorax. Therefore, the objective of this study was to explore rib variability in strain magnitude, rates, and modes between levels 3-8 in dynamic frontal loading tests in multiple tissue states.

I. METHODS

Experimental Setup and Testing

A series of non-injurious frontal thoracic impacts were conducted at 3m/s on five male PMHS [22]. Subjects were approximately 50th percentile males for height and weight and ranging from 55-73 years old. A summary of each subjects' anthropometric measurements and demographics are listed in Table I. A fixed-back set-up (Fig. 1) was utilized in order to measure chest deflection and match the boundary conditions of the individual rib testing. The backs of each PMHS were positioned flush against the posterior plate by a lap belt holding the pelvis firmly in place and a head halter to suspend the head in position. The anterior thorax of each subject was impacted by a pneumatic ram with a 24kg rectangular impactor face (15.2cm height x 30.5cm width x 1.3cm depth). Chest depth was measured prior to each impact, and chest deflection was limited to <20% in order to remain non-injurious. The impactor was centered on the superior and inferior aspects of the sternum of each subject in order to engage mid-level ribs (3-8). Prior to all testing, uniaxial strain gauges (Vishay Micro-Measurement, CEA-06-062UW-350, Sheldon, CT, USA) were attached to the cutaneous surfaces along the long axis of left and right ribs 3-8 at 30% (posterior) and 60% (anterior) of the rib curve length. Soft tissue and periosteum were cleared only at the site where the gauge was applied. Strain gauges were glued to the surface and sealed to prevent moisture entering the site throughout the testing series. Additional details on the experimental set-up can be found in [7,22]. All strain and kinematic data channels were recorded at 20,000 Hz using TDAS G5 and SLICE PRO data acquisition systems (Diversified Technical Systems, Seal Beach, CA, USA).

In order to test the thoraces in a hierarchical manner, each subject was impacted once in three subsequent tissue states: intact, denuded, and eviscerated. The denuding process included removal of the upper limbs while the clavicles were kept intact, removal of subcutaneous tissue, and superficial thoracic muscles. The eviscerated thorax was tested after all abdominal and thoracic viscera as well as the diaphragm muscle were removed. Prior to the eviscerated test, strain gauges were also attached to the pleural surfaces of levels 3-8 at matched locations of the cutaneous gauges. Figure A1 provides exemplar impactor acceleration and velocity curves from the three tissue states to demonstrate the impact boundary conditions prior to impact. The impact velocity of 3 m/s immediately prior to contacting the thorax was utilized to produce a strain rate of 0.5 strains/s. This is the same strain rate as individual rib testing and accomplishing the rate in the thorax was verified by previous work on impact velocities and strain rates in this loading direction with this test set-up [23]. Throughout the testing series, elastic deformation was monitored to ensure strains returned to zero after each loading cycle was complete and no plastic deformation was seen. Intrinsic back muscles and intercostal muscles remained intact across all tissue states. Fig. 1a-c shows an example of PMHS E across all three tissue states. Prior to each impact, chest depth was

measured in the seated position to calculate the target chest deflection required for the tests to remain non-injurious.

Individual Rib Testing

After eviscerated testing was complete, left and right ribs of levels 4-7 were removed and tested in a dynamic simplified anterior-posterior bending scenario. These ribs were tested to failure in a custom-built pendulum fixture simulating a frontal impact where the sternal end of the rib was translated towards the vertebral end at 2m/s which corresponds to an average strain rate of 0.5 strain/s. The strain gauges instrumented during thorax testing were kept in place for rib testing in order to obtain strain data at comparable locations. Additional details on sample preparation and experimental testing have been described in [10].

TABLE I
ANTHROPOMETRY OF ALL MALE SUBJECTS

	PMHS A	PMHS B	PMHS C	PMHS D	PMHS E	Avg. ± 1 SD.	50th Percentile Male [24]
Age (yrs)	73	62	55	70	59	64 ± 7.5	N/A
Mass (kg)	62	84	75	79	65	73 ± 9.3	77
Stature (cm)	170	173	183	191	180	179 ± 8.3	175
BMI (kg/cm^2)	21	28	22	22	20	23 ± 3.2	25
Chest Depth (cm)	25	26	22	25	20	24 ± 2.5	22
Chest Breadth (cm)	33	34	32	33	35	34 ± 1.1	23
Chest Circumference (cm)	90	108	95	105	92	98 ± 8.0	97

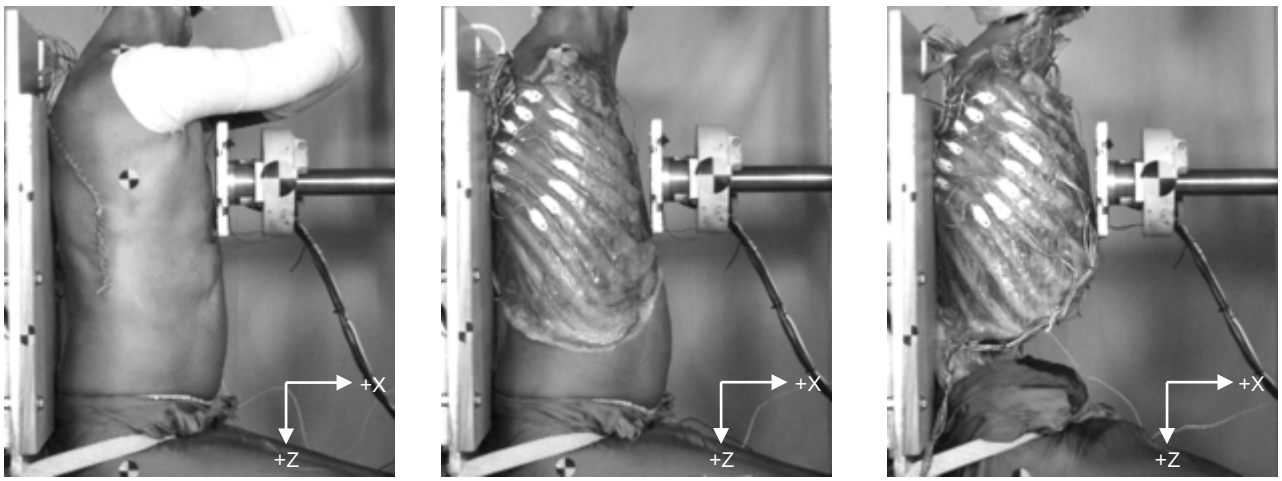

a. Intact b. Denuded c. Eviscerated

Fig. 1. PMHS E in thoracic hierarchy experimental set-up in three tissue states: a. Intact, b. Denuded, c. Eviscerated. PMHS were positioned in a fixed back set-up with strain gauges on levels 3-8 at 30% (posterior) and 60% (anterior) locations.

Data Processing and Analysis

Strain modes were determined by analyzing strain vs. time curves where tension was identified by the positive profiles and compression was identified by the negative profiles. Fig. 2a shows strain vs. time curves of ribs 3-8 at the anterior gauge site on the cutaneous surface from an exemplar intact thorax test. Fig. 2b shows strain vs. time curves of ribs 4-7 at the anterior cutaneous surface from individual rib testing. Peak strain was defined as the maximum absolute strain recorded by the gauges. Strain data were then filtered using the channel filter class, CFC180 [25], to calculate peak strain rate by identifying the maximum value when differentiating filtered strain

over time. Left and right ribs were accounted for as individual observations when rib-level averages were computed. Analysis of variance (ANOVA) was used to evaluate differences in peak strain and peak strain rates between rib levels across tissue states and subjects. To focus on rib-level variation and to obtain statistically significant amount of observations, tissue states and subjects were combined in order to identify significant differences. Tukey's test was further utilized to identify which specific comparisons were significant for post hoc analysis.

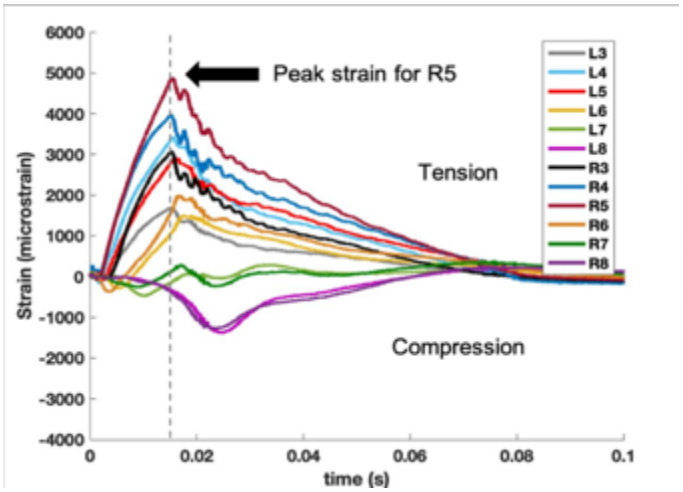

Fig. 2a. Exemplar strain vs. time curves of ribs 3-8 of PMHS E on the cutaneous surface at the anterior site from an intact thorax test. Paired shades of colors represent right and left ribs. Peak deflection occurred at 0.014s for this test as denoted by the dashed gray line.

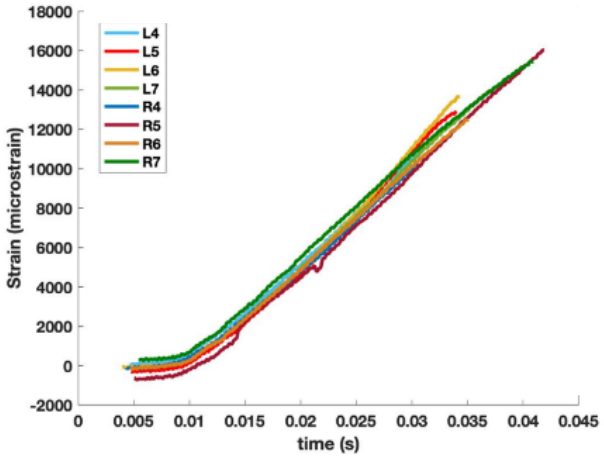

Fig. 2b. Exemplar strain vs. time curves of ribs 4-7 from individual rib testing of ribs from PMHS E. Paired shades of colors represent right and left ribs. The gauges here are only from the cutaneous surface of the anterior site.

II. RESULTS

Thorax Testing - Strain Modes on Cutaneous Surfaces

Strain modes were identified by rib level for each subject. For all PMHS, levels 3-6 consistently demonstrated tension in all tissue states for cutaneous gauges at the anterior location and posterior locations. While the primary strain mode of ribs levels 3-6, was tension on the cutaneous surfaces, these levels initially showed brief compression on the cutaneous surface close to time zero when the ribs were in contact with the impactor face. The strain profiles and initial loading behavior were very similar for rib levels 3-6. Level 7 demonstrated both compression and tension over time on the cutaneous surface while level 8 was predominantly in compression at both sites. These trends stayed consistent over tissue states. While rib levels 3-6 were directly engaged with the impactor face, rib level 8 showed compression on the cutaneous surface at the anterior and posterior locations with higher strain magnitudes of compression at the posterior than the anterior location in PMHS B, C, D, and E. PMHS A did not exhibit this phenomenon at the eighth rib level.

Thorax Testing - Peak Strain Magnitudes

Peak strain was identified for each rib level across tissue states. In order to account for peak strains in both tension and compression modes, absolute peak strain was analyzed. Comparisons of each rib level by tissue state are presented as an average of all subjects at the anterior gauge location (Fig. 3a). Rib-level comparisons by tissue state of each subject are shown in Fig. A2. Peak strain values are tabulated in Table AI for all subjects. Peak strains were generally greater in the intact tests compared to other tissue states across all rib levels. A general reduction in peak strain was observed across rib levels as tissue was removed. Highest peak strains were seen in rib levels 4-6, across subjects. Levels 7 and 8 consistently experienced lower peak strain values than levels 4-6 in all tissue states, likely because these ribs were not directly in contact with the impactor face like levels 4-6 were.

Fig. 3b provides comparisons of each rib level by tissue state, averaged from all subjects, at the posterior gauge location. Fig. A3 shows the same comparison for each subject. Peak strain values are catalogued in Table AII for all subjects. The posterior gauges demonstrated lower absolute peak strain magnitudes than the anterior location in levels 3-7. However, at level 8 posterior locations exhibited greater strain than anterior locations across tissue states. The variation in peak strain by tissue state at the posterior location is lower, indicated by the smaller standard deviation as compared to anterior location, for all levels in all subjects. Denuded tissue states exhibited higher average peak strains in the posterior location compared to other tissue states, but this trend was only marginally higher in comparison to the intact tests. Peak strains generally occurred at peak deflection and Table AIII has maximum compression and chest depths tabulated for each subject.

Descriptive statistics for cutaneous peak strain at the anterior and posterior location across rib levels can be found in Table AIV. Significant differences were found in anterior peak strain (ANOVA, $p<0.0001$) across rib levels. Post hoc tests revealed that peak strains in rib levels 7 and 8 were significantly lower from levels 3-6, and level 4 was significantly higher than levels 3 and 6-8. However, levels 3 and 6 were not significant from each other and 5 was not significantly higher or lower than 4-6 (Fig. 4a-b). Significant differences were found in posterior peak strain (ANOVA, $p<0.0001$) across rib levels. Peak strain in the 8th level was significantly higher from all levels except 5 as demonstrated from post hoc tests. Levels 3-7 demonstrated similar means and were not found to have posterior peak strains significantly higher or lower from each other (Fig. 4c-d). Differences in pleural peak strain values were not evaluated as these gauges were only present in the eviscerated tests.

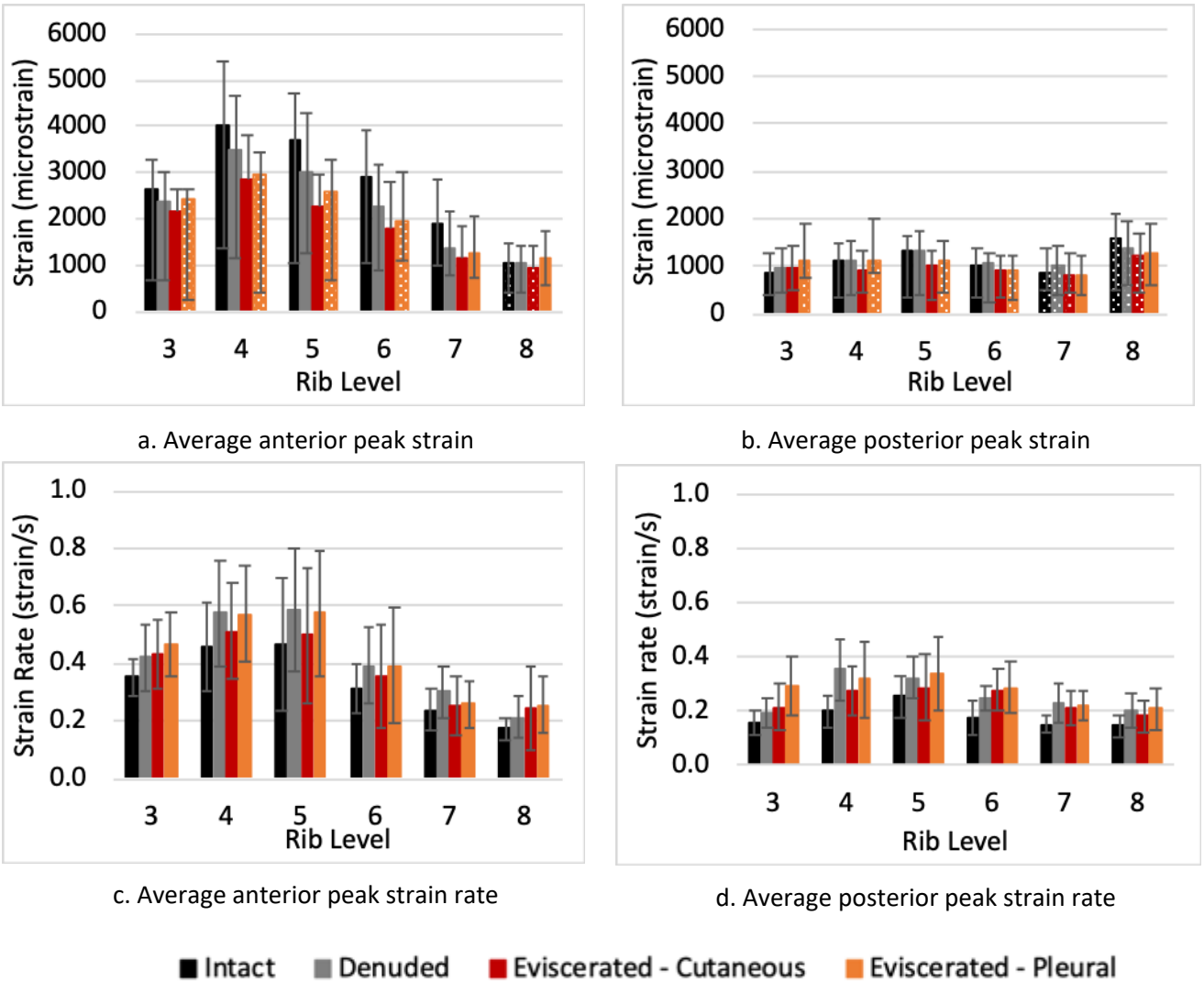

a. Average anterior peak strain

b. Average posterior peak strain

c. Average anterior peak strain rate

d. Average posterior peak strain rate

Fig. 3. Absolute peak strain (a,b) and peak strain rate (c,d) presented as averages by rib level for PMHS A-E in intact, denuded and eviscerated tissue states from the cutaneous surface gauges. Orange bars represent pleural surface gauges from the eviscerated tests. Gauges are from anterior location (a,c) and posterior location (b,d). One standard deviation is denoted for each bar. Patterned bars represent compression mode.

Thorax Testing - Peak Strain Rate

Fig. 3c and 3d compare average peak strain rates of all subjects by rib level across tissue states at the anterior and posterior gauge site. Tables AV and AVI tabulate absolute peak strain rate at anterior and posterior gauge locations, respectively, for all subjects. Descriptive statistics for peak strain rates at the anterior and posterior cutaneous locations can be found in Table AVII. Higher peak strain rates were observed in the anterior locations, particularly levels 3-5, than the posterior locations (Paired T-Test, $p<0.0001$). Significant differences were observed in peak strain rates at the anterior location between rib levels (ANOVA, $p<0.0001$). Post hoc tests revealed that peak strain rates in levels 6-8 were significantly lower than levels 4-5, but no different from level 3. Additionally, peak strain rates in level 5 were significantly higher than level 3 but not 4, and levels 3 and 4 were not significantly different from each other (Fig. 5a-b). This is intuitive as the impactor plate was centered on the sternum during impact, engaging ribs 4-5 directly. Significant differences were revealed in peak strain rates at the posterior location across rib levels as well (ANOVA, $p<0.0001$). Post hoc tests demonstrated that peak strain rates in rib levels 3 and 6-8 were lower than levels 4-5 (Fig. 5c-d). In all ribs, strain rates generally increased as tissue was removed at both locations.

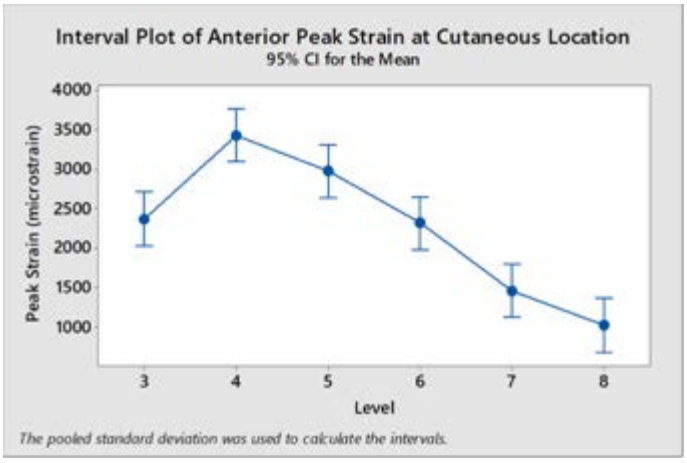

a. Anterior peak strain

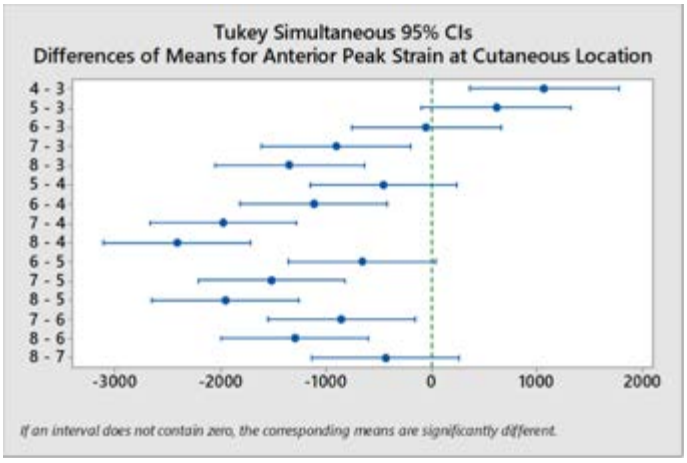

b. Post hoc test for anterior peak strain

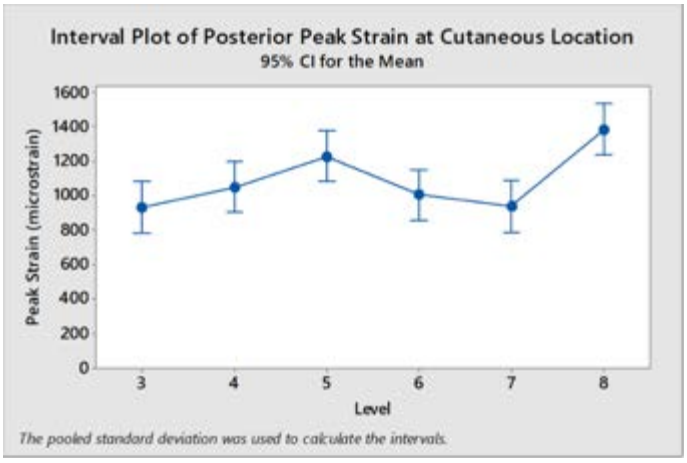

c. Posterior peak strain

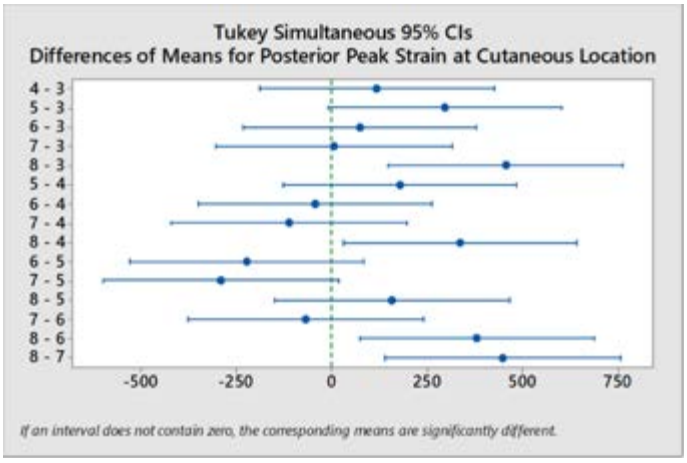

d. Post hoc test for posterior peak strain

Fig. 4. 95% CI for peak strain at anterior (a) and posterior (b) cutaneous locations from thorax tests. Post hoc tests show which differences are significant in peak strain across rib levels at the anterior (b) and posterior locations (d).

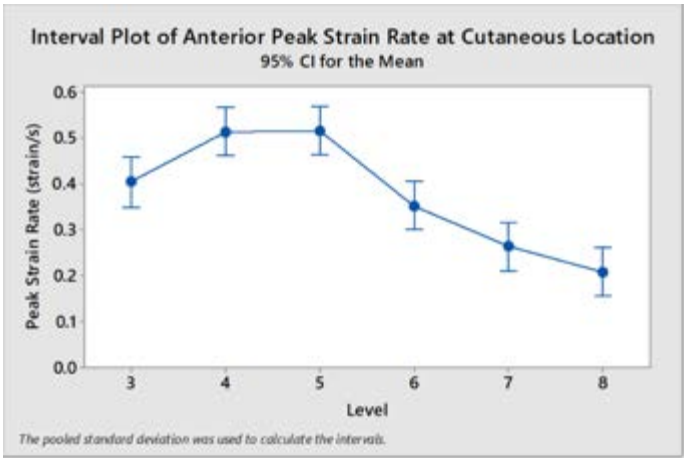

a. Anterior peak strain rates

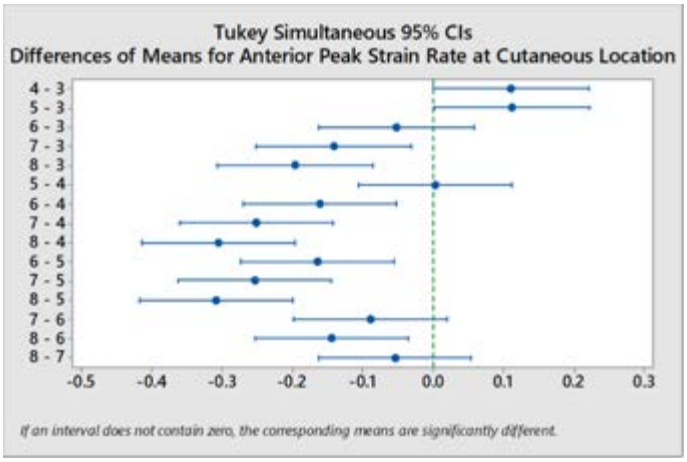

b. Post hoc test for anterior peak strain rates

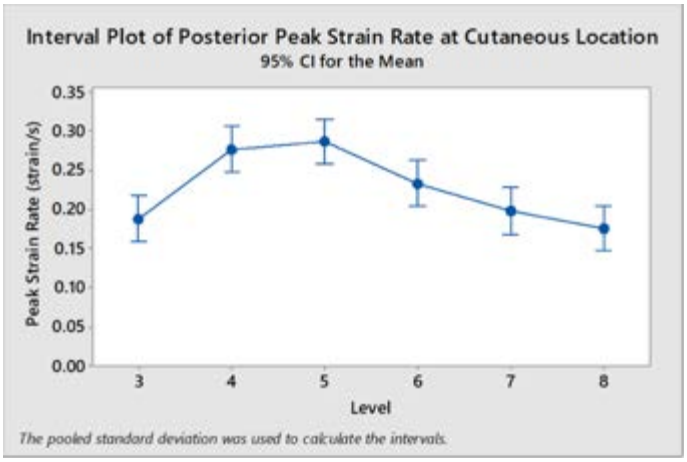

c. Posterior peak strain rates

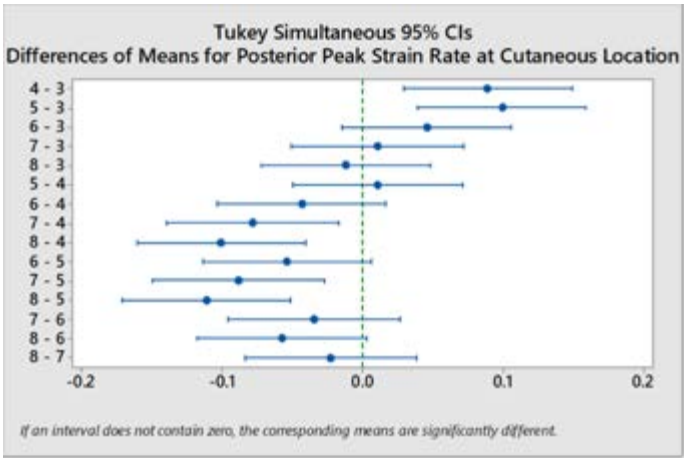

d. Post hoc test for posterior peak strain rates

Fig. 5. 95% CI for peak strain rate at anterior (a) and posterior (c) cutaneous locations from thorax tests. Post hoc tests show which differences are significant in peak strain rates across rib levels at the anterior (b) and posterior locations (d).

Thorax Testing - Cutaneous vs. Pleural Behavior

In the eviscerated tissue state, the ribs were instrumented both on the cutaneous and pleural surfaces at anterior and posterior locations. Strain profiles show that the cutaneous and pleural surfaces for each rib follow similar deformation patterns (Fig. 5), but with opposite polarity. Peak strain magnitudes were generally greater on the pleural surfaces than cutaneous surfaces at the anterior gauge. The opposite was true for the posterior gauge across rib levels. This behavior can be seen by the comparisons of the red and orange bars in Fig. 3. Peak strain rates demonstrated the opposite observation where the anterior locations on the cutaneous surfaces were greater than pleural surfaces for all rib levels. However, peak strain rates were similar in the cutaneous and pleural surfaces at the posterior site and demonstrated less variation.

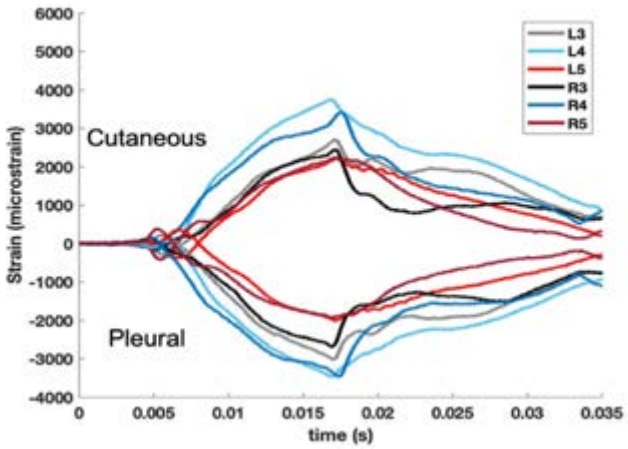

Fig. 5. Strain profiles from cutaneous and pleural surface gauges at the anterior location for rib levels 3-5 from an eviscerated thorax test. Cutaneous surface gauges show positive profiles while pleural gauges show negative profiles.

Thorax Testing - Inter-subject Variation

Comparisons of rib level 5 across tissue states for each subject are in Fig. 6. To evaluate inter-subject variation, peak strain and were compared for rib level 5 as this level was best aligned with the center of the impactor face vertically. Peak strain magnitudes show larger variation in each tissue state across subjects at the anterior site than posterior site. PMHS A and B generally exhibited lower peak strain magnitudes in the anterior location than PMHS C, D and E. This demonstrates that while the same rib level was selected as a common comparison across tissue states, strain magnitudes are different across subjects for each tissue state.

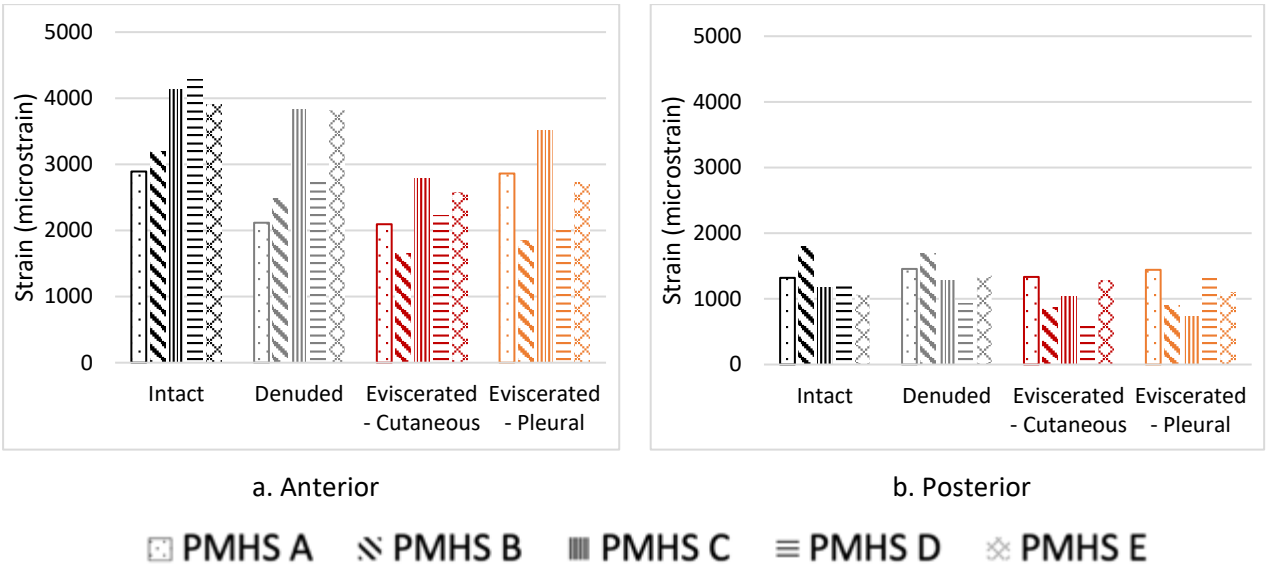

Fig. 6. Comparison of peak strain at rib level 5 of all subjects across tissue states at the anterior location (a) and posterior location (b). Rib level 5 experienced tension in the intact, denuded, and eviscerated conditions at the cutaneous locations. Pleural locations during the eviscerated tests demonstrated compression.

Individual Rib Testing

After the eviscerated thorax testing was completed, bilateral rib pairs of levels 4-7 were removed and individually tested to failure in dynamic anterior-posterior bending. The strain modes observed were the same across all rib levels where cutaneous surfaces experienced tension and pleural surfaces experienced compression at anterior and posterior gauge locations. Fig. 7a-b compares peak strain by rib level at the anterior and posterior gauge locations. Tables AVIII contain peak strain for each rib tested from all subjects.

Peak strains experienced by every rib were relatively high in magnitude as these ribs were tested to failure unlike the non-injurious compression limit used in the thorax tests. At the anterior and posterior location, peak strains generally increased in rib levels 4 to 7 on cutaneous and pleural surfaces. No significant differences in peak strain were found between rib levels at the anterior (ANOVA, p=0.17) or posterior (ANOVA, p=0.79) location as shown in Fig. 7. Descriptive statistics for cutaneous peak strain at the anterior and posterior locations across rib levels can be found in Table AIX. The testing scenario was designed to achieve a strain rate of 0.5 strain/s during individual rib testing and resultant peak strain rates observed were close to 0.5 strain/s across all ribs. No significant differences in peak strain rates were found between rib levels at the anterior (ANOVA, p=0.19) or posterior (ANOVA, p=0.62) location on the cutaneous surfaces. Average peak strain rates for all rib levels were 0.52 ± 0.12 strain/s at the anterior location and 0.51 ± 0.13 strain/s at the posterior locations.

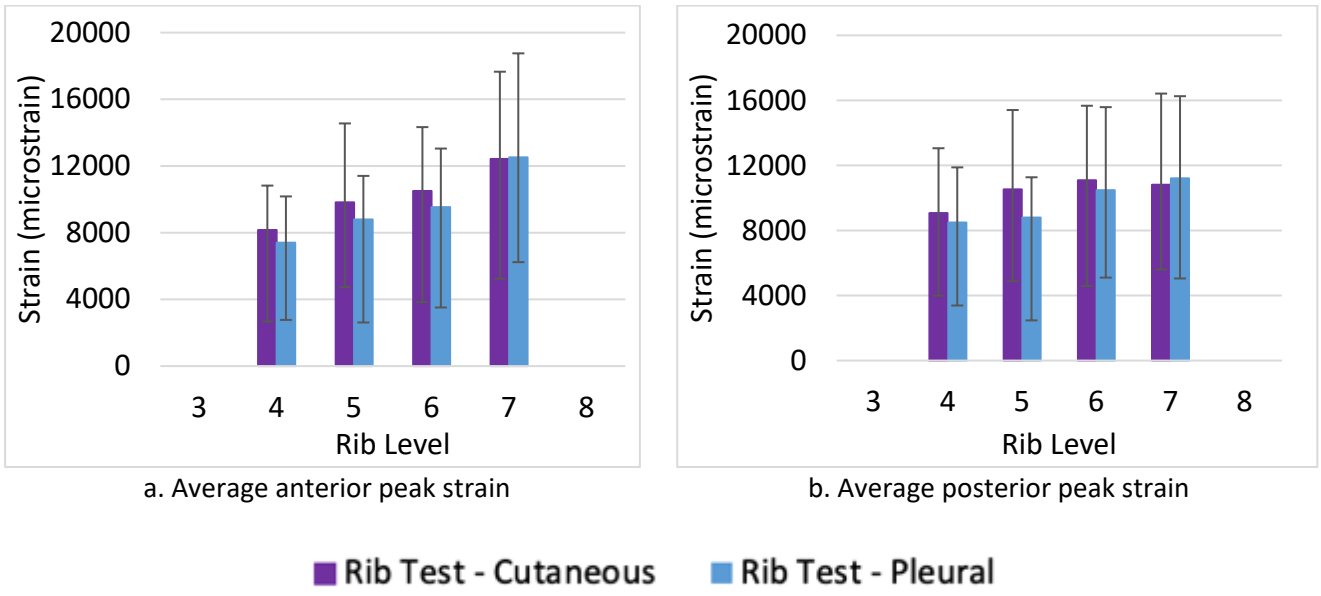

a. Average anterior peak strain

b. Average posterior peak strain

Fig. 7. Absolute peak strain presented as averages by rib level across all individually tested ribs from all 5 PMHS. Gauges are from anterior locations (a) and posterior locations (b). Cutaneous data are always in tension and pleural always in compression. One standard deviation is denoted for each bar.

Thorax Testing vs. Individual Rib Testing

While the boundary conditions used in the thorax testing were aimed at mimicking the set-up of individual rib testing, the severity of the full thorax and rib tests were different. The thorax tests were conducted up to 20% deflection while individual rib tests were tested to failure. Since the magnitudes of peak strain and strain rates from the thorax and individual rib tests cannot be compared directly due to these differences, percent differences of average peak strain between rib levels were calculated for both the thorax tests and rib tests to further explore rib-level comparisons. Fig. 8a-b shows these comparisons of percent differences in peak strain at the anterior and posterior locations between rib levels.

Thorax tests resulted in greater differences between rib levels than in the individual rib tests. Intact thorax tests generally resulted in higher percent differences between rib levels in peak strain at both anterior and posterior locations than other tissue states. Percent differences in peak strain observed between levels 6 to 7 at the anterior

location and between 7 to 8 at the posterior location were greater than differences between other levels in the thorax tests. Differences in peak strain between levels 6 to 7 were greater in individual rib tests at the anterior location on the cutaneous surface but levels 4-5 displayed larger percent differences at the posterior location compared to other levels. No significant differences in strain magnitudes between rib levels were found when percent differences were assessed at the anterior locations (ANOVA, p=0.090) but significant differences were found at the posterior locations (ANOVA, p=0.0004). Fig. 9a-b show the interval plots for anterior and posterior percent differences. Post hoc tests revealed that percent differences between levels 7-8 were higher than the other rib levels at the posterior location.

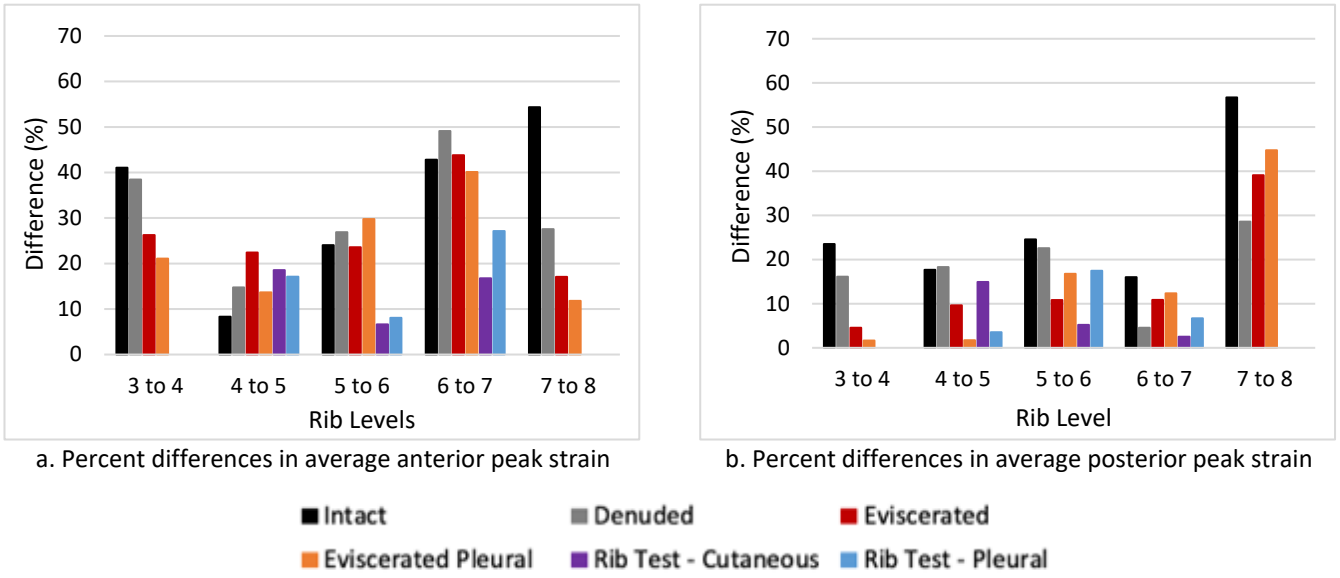

a. Percent differences in average anterior peak strain

b. Percent differences in average posterior peak strain

Fig. 8. Peak strain expressed as percent differences by rib level for all tissue states from thorax testing and individual rib testing from anterior (a) and posterior (b) locations. Orange and blue bars represent pleural gauges.

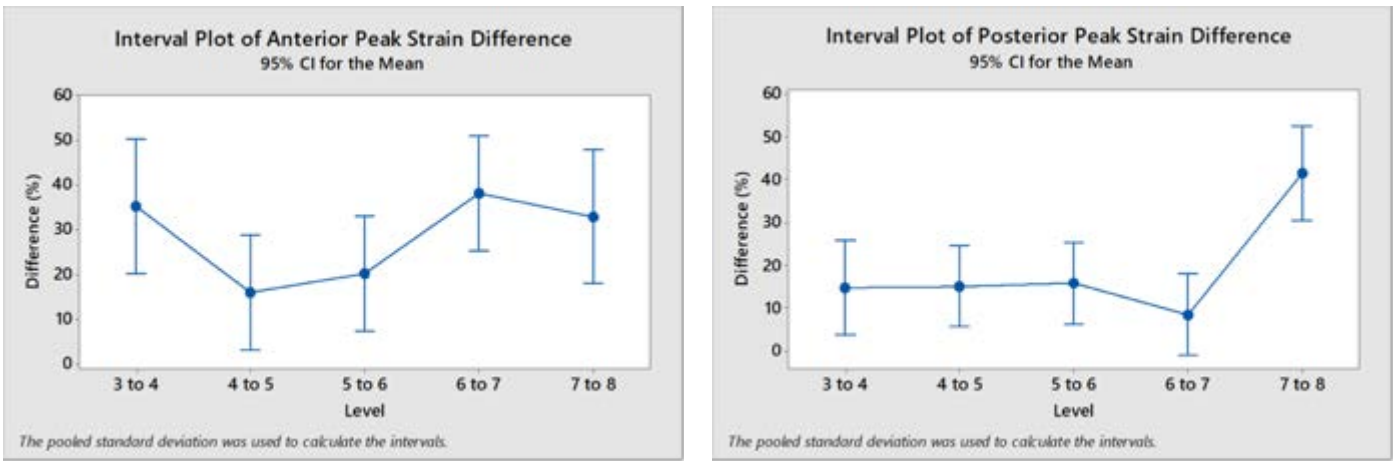

a. 95% CI for Anterior peak strain difference (%)

b. 95% CI for Posterior peak strain difference (%)

Fig. 9. 95% CI for anterior (a) and posterior (b) peak strain difference (a) at the cutaneous location from all tests (thorax and individual rib tests).

III. Discussion

The primary objective of this study was to explore strain modes, magnitudes, and rates in rib levels 3-8 with a focus on various tissue states to assess local deformation patterns of the thorax in dynamic, distributed loading

and explore differences at the component level with dynamic individual rib testing. While previous studies have investigated each of these aspects separately (tissue states, rib strain, and various loading types), this study attempts to combine these factors to gain a better understanding of thorax strain distributions in response to applied loads.

Understanding strain modes of the different rib levels was the first step in categorizing the bending observed during frontal loading of the thorax. The current study found that while rib levels 3-6 experienced tension on the cutaneous surface, 7th level ribs did not consistently display one strain mode, instead behaving as a mode transition zone between superior and inferior ribs. Eighth level ribs generally experienced compression at the cutaneous location. Previously conducted dynamic thorax tests, utilizing a hub impactor face in a frontal loading direction, found that cutaneous rib strain profiles at levels 3-5 were in tension in levels, level 6 ribs had varying modes, and level 7-9 ribs were in compression [26]. The results from both of these studies have demonstrated that all rib levels may not have the same strain mode and deformation mechanism and that these modes and mechanisms are highly dependent on impactor geometry. The transition from tension to compression in strain modes between levels could be different in other loading types (i.e. airbag loading and diagonal loads such as a seatbelt). A frontal airbag loading scenario would likely demonstrate similar strain modes as the impactor used in this study, since the distributed loading is similar. However, the loading from a shoulder belt would be less distributed and instead applied diagonally across the thorax, so therefore the same trends in strain modes might not occur. From the literature, it is known that the shoulder and upper torso bear most of the structural loads during various loading scenarios (i.e. seatbelt loading) to the thorax [1]. While a similar strain profile in these regions could be observed, if further testing in different loading scenarios is conducted, the strain modes might be different between the superior and inferior level ribs. These differences between strain modes in rib levels need to be considered when assigning rib-specific properties and evaluating the biofidelity of computational HBMs by comparing strains observed in models against strains measured in experimental testing.

Differences between rib levels were explored via structural coupling in a previous study conducted at quasi-static loading rates [17]. Specifically, superior ribs were found to be more coupled in the thorax than the inferior level ribs in the rib cage. While investigating the coupling of the individual ribs in dynamic loading scenarios was difficult in this study due to the distributed frontal load being applied across levels 3-6, a similar deformation trend was still observed likely due to these ribs being directly connected to the sternum. While the superior level ribs, levels 3-6, were directly engaged with the impactor, inferior ribs, at levels 7-8, though not in contact with the impactor, experienced strain at lower magnitudes and often in the opposite strain mode. This suggests that the connections of the ribs via the intercostal muscles, sternum, and costal cartilage link the ribs in a predictable manner and play a role in overall thorax deformation. Peak strains generally occurred at maximum compression of the thorax, but this was not a consistent observation demonstrated across all rib levels and subjects. This was likely due to inertial effects and the delayed peak strain behavior across rib levels as a result of the impact. Future work will include assessing differences in peak strain times in relation to peak deflection times to further quantify the loading and unloading of the thorax.

In addition to coupling observed within the bony thorax, coupling of the bony thorax to the musculature and skin also had an effect on the strain behavior of each rib. It was expected that rib peak strain would increase with the removal of tissue as the bony thorax would come directly in contact with the linear impactor without potential damping effects from soft tissue. However, this theory was not supported, as peak strains in the intact tissue state were generally found to be greater at the anterior location in all rib levels. This suggests that the lack of tissue potentially caused the ribs to experience other outlets of deformation, such as rotation about the costovertebral joint or off-axis strains near the impact site. Future work will focus on quantifying deformations outside of the main loading axis.

The opposite trend was observed in peak strain rates where the removal of tissue showed an increase in strain rates across rib levels in the anterior location. While the peak strains were greater in the intact condition, eviscerated tests showed higher peak strain rates indicating that the contributions of the external skin and musculature play a role in the rate of deformation of the ribs and in protection of the bony thorax. On the contrary, it can be argued that the thoracic and abdominal viscera provide support to the internal surface of the bony thorax and the lack of this internal support resulted in higher deformation rates in the eviscerated tests. Cutaneous and pleural behavior in the eviscerated thorax was also studied across rib levels and it was found that pleural surfaces generally experienced marginally higher strain at the anterior location. This could be due to the

geometry of the ribs and perhaps the pleural surfaces having to resist combined loads in the opposite strain mode as the polarity of the applied load. Pleural surfaces experienced a combination of bending and compression strains when anteriorly loaded. The polarities of the combined load likely were both negative and therefore resulted in higher peak strains. Strain modes on the pleural and cutaneous surfaces along the length of the rib need to be further explored and taken into consideration when translating these results to models.

This current study focused on investigating 50th percentile males based on height and weight. Comparing rib levels across tissue states, the peak strain magnitudes were highly variable indicating that all subjects even in the same demographic may not have the same thorax behavior. Previous component level testing of individual ribs demonstrated that age, sex, and body size did not accurately predict rib response and that other factors need to be explored to explain the variation in structural properties [10,27]. Similarly, the variation in strain magnitudes seen across rib levels of thoraces in the five 50th percentile male subjects likely follow the same complexity. Additional factors, such as overall geometry of the thorax and rib angles within the thorax, need to be explored between subjects to quantify the differences seen in peak strain magnitude. The degree of variation in peak strain values indicates the importance of characterizing various elastic-plastic deformation limits in ribs for all demographics.

The intent of the hierarchical approach taken to experimentally test subjects was to explore ribs in the whole thorax and also study the individual rib behavior when dynamically loaded in an anterior-posterior bending scenario. Individual rib testing demonstrated that differences in failure tolerance exist at every rib level since average peak strain values varied in rib levels 4-7. These trends were different in thorax testing where rib levels 4 and 5 showed higher peak strain values than the other levels and levels 6-8 showed lower peak strains as well as different strain modes than levels 3-5. These differences in rib levels between types of testing likely occurred because of the lack of direct engagement of inferior ribs with the impactor during thorax tests. The individual ribs were fully engaged during simplified anterior-posterior loading and were loaded in plane and along the long axis of the rib. Percent differences in average peak strains by rib levels revealed that thorax tests demonstrated greater differences in strain between rib levels than in individual rib tests. This is likely because the boundary conditions of the individual rib tests provide a more controlled bending scenario whereas the thorax testing engagement levels differ. Additionally, the intact thorax tests revealed greatest percent differences in peak strain across most rib levels at the anterior and posterior locations indicating that soft tissue and viscera play a role in rib level deformation. This highlights the critical need to explore all components of the thorax, not just the bony thorax, and their contributions to local deformation in relation to load distributions.

This study revealed important rib-level deformation trends in dynamic frontal loading scenarios, but there were limitations to the experimental testing. The angled thorax was impacted with the straight plate, engaging the ribs at different levels at different times. The boundary conditions of thorax testing included a rigid, fixed-back set-up which could have restricted the rib's deformation in posterior locations. Additionally, the strain modes and magnitudes experienced at the posterior location of the rib levels 7 and 8 could be influenced by the rigid, fixed-back support. The effects of the sternum and costal cartilage were not evaluated in this study and in order to understand the thorax further, these contributions should be studied in future work. This testing series was designed to be non-injurious as chest deflection in each tissue state was limited to 20% of the chest depth for each tissue state. However, four incomplete rib fractures occurred in PMHS C and five incomplete fractures occurred in PMHS E. These fractures were not detected from strain gauge data, likely because these fractures were incomplete fractures very close to the costochondral junction and no visible changes in strain profiles were observed. Identification of rib fractures at a low chest deflection limit suggest that due to the heterogeneity of bone, other factors such as differences in structural or material properties of the ribs themselves may have had an influence in causing these injuries. Additionally, there is a possibility that these fractures were pre-existing and could explain why these fractures were not detected by the strain gauges.

The overall goal of the hierarchical testing was to characterize various components of the thorax to understand thoracic deformation mechanisms. The data provided in this study was a first step in understanding the strain distributions by rib level at different locations, while maintaining the structural integrity of the thorax and exploring the same distributions in the individual ribs when tested by themselves. Future work will explore how individual rib responses can be used to predict the response of the intact thorax. Exploring this connection from the individual rib to all tissue states of the thorax will help bridge the gap in understanding how the rib fits into the context of the thorax. By understanding this rib-thorax connection, a strain-based model may be constructed

to predict the intact thoracic response based on rib characteristics.

IV. CONCLUSIONS

This study provides preliminary data at understanding rib-level deformation in various tissue states in the context of the whole thorax. It was determined that rib levels 3-6 exhibited different strain modes and peak strain magnitudes across subjects from levels 7-8. Localized deformation by rib level provides valuable insight into further understanding the thorax by breaking it down to various tissue states. These results in parallel with an expansive dataset of individual rib properties and thoracic response can be used to develop a strain-based model. Data presented in this study can also be used to assign accurate rib-level properties and load distributions to obtain desired local deformation across the thorax to improve the biofidelity of computational human body models.

V. ACKNOWLEDGEMENT

Thank you to the anatomical donors for their generous donations and for making this research possible. Thank you to the National Highway Traffic Safety Administration (NHTSA) for sponsoring this research. The views presented in this study are those of the authors and do not represent those of NHTSA. We are grateful to the students and staff of the Injury Biomechanics Research Center especially Julie Mansfield, Arrianna Willis, David Stark, Yadetsie Zaragoza-Rivera, Scott Stuckey, Victoria Dominguez, Angela Harden, and Reagan Di Iorio, for assisting in test preparation and data collection.

VI. REFERENCES

[1] Kent, R. (2008) Frontal thoracic response to dynamic loading: The role of superficial tissues, viscera and the rib cage. *International Journal of Crashworthiness* **13**(3):289-300.

[2] Kent, R., Lee, S. *et al.* Structural and material changes in the aging thorax and their role in crash protection for older occupants. *Stapp Car Crash Journal* **49**:231-249.

[3] Forman, J., Poplin, G.S., et al. (2019) Automobile injury trends in the contemporary fleet: Belted occupants in frontal collisions, *Traffic Injury Presentation*, 2**0**(6):607-612.

[4] Viano, D.C., Lau, V.K. (1983) Role of impact velocity and chest compression in thoracic injury. *Aviation Space and Environmental Medicine* **54**(1):16-21.

[5] Kroell, C.K., Pope, M.E., Viano, D.C., Warner, C.Y., Allen, S.D. (1981) Interrelationship of velocity and chest compression in blunt thoracic impact. *Stapp Car Crash Journal* **25**:549-579.

[6] Kent, R.W., Crandall, J.R., Bolton, J., Prasad, P., Nusholtz, G., Mertz, H. (2001) The influence of superficial soft tissues and restraint condition on thoracic skeletal injury prediction. *Stapp Car Crash Journal* **45**:183-204.

[7] Ramachandra, R., Kang, Y.S., *et al.* Evaluation of skeletal and soft tissue contributions to thoracic response of GHBMC M50-O model in dynamic frontal loading scenarios. *Proceedings of IRCOBI Conference,* 2019, Florence, Italy.

[8] Pipkorn, B., and Kent, R. Validation of a human body thorax model and its use for force and strain analysis in various loading conditions. *Proceedings of IRCOBI Conference.* 2011. Krakow, Poland.

[9] Albert, D.L., Kang, Y.S., Agnew, A.M., Kemper, A.R. The effect of injurious whole rib loading on rib cortical bone material properties. *Proceedings of IRCOBI Conference,* 2018, Athens, Greece.

[10] Agnew, A.M., Murach, M.M., *et al.* (2018) Sources of variability in structural bending response of pediatric and adult human ribs in dynamic frontal impacts. *Stapp Car Crash Journal* **62**:119-192.

[11] Cormier, J.M., Stitzel, J.D., Duma, S.M., Matsuoka, F. Regional variation in the structural response and geometrical properties of human ribs. *Proceedings of Associate for the Advancement of Automotive Medicine*, 2005, Cambridge, Boston.

[12] Yoganandan, N., Pintar, F. (1998) Biomechanics of human thoracic ribs. *Journal of Biomechanical Engineering* **120**(1):100-105.

[13] Kemper, A.R., McNally, C., *et al.* (2007) The biomechanics of human ribs: material and structural properties from dynamic tension and bending tests. *Stapp Car Crash Journal* **51**:235-273.

[14] Kalra, A., Saif, T., *et al*. (2005) Characterization of human ribs biomechanical responses due to three-point bending. *Stapp Car Crash Journal* **59:**113-130.

[15] Murach, M.M., Kang, Y.S. *et al.* (2017) Rib geometry explains variation in dynamic structural response: potential implications for frontal impact fracture risk. *Annals of Biomedical Engineering* **45**(9): 2159-2173.

[16]Schafman, M.A., Kang, Y.S., Moorhouse, K., White, S.E., Bolte, J.H. IV, Agnew, A.M. (2016) Age and sex alone are insufficient to predict human rib structural response to dynamic A-P loading. *Journal of Biomechanics* **49**(14):3516-3522.

[17]Kindig, M.W., Lau, A.G., Forman, J.L., Kent, R.W. (2010). Structural response of cadaveric ribcages under a localized loading: Stiffness and kinematic trends. *Stapp Car Crash Journal* **54**:337-380.

[18]Vezin, P. and Berthet, F. (2009) Structural characterization of human rib cage behavior under dynamic loading. *Stapp Car Crash Journal* **53**:93-125.

[19]Baudrit, P., Petitjean, A., Potier, P., Trosseille, X., Vallencien, G. (2014) Comparison of the thorax dynamic responses of small female and midsize male post mortem human subjects in side and forward oblique impact tests. *Stapp Car Crash Journal* **58**:103-121.

[20]Ali, T., Kent, R.W., Murakami, D., Kobayashi, S. (2005) Tracking rib deformation under anterior loading using computed tomography imaging. *SAE International*: 111-125.

[21]Kemper, A. R., Kennedy, E. A., McNally, C., Manoogian, S. J., Stitzel, J. D., Duma, S. M. (2011) Reducing chest injuries in automobile collisions: Rib fracture timing and implications for thoracic injury criteria. *Annals of Biomedical Engineering* **39**(8):2141-2151.

[22]Murach, M.M., Y.S. Kang, et. al (2018). Quantification of soft tissue and skeletal contributions to thoracic response in a dynamic frontal loading scenario. *Stapp Car Crash Journal* **62**:193-269.

[23]Shurtz, B.K., Agnew, A.M., Kang, Y.S., Bolte, J.H. IV (2017) Effect of chestbands on the global and local response of the human thorax to frontal impact. *Annals of Biomedical Engineering* **45**(11): 2663-2672.

[24]Robbins, D.H. (1983) University of Michigan, *Anthropometric specifications for mid-size male dummy* volume 2, Ann Arbor, MI, USA.

[25]SAE (2007). *Instrumentation for Impact Test-Part 1 – Electronic Instrumentation, J211/1.* Warrendale, PA.

[26]Trosseille, X., Baudrit, P., Leport, T., Vallancien, G. (2008) Rib cage strain pattern as a function of chest loading configuration. *Stapp Car Crash Journal* **52**:205-231.

[27]Agnew, A.M., Murach, M.M., Misicka, E., Moorhouse, K., Bolte, J.H. IV, Kang, Y.S. The effect of body size on adult human rib structural properties. *Proceedings of IRCOBI Conference*, 2017, Antwerp, Belgium.

VII. APPENDIX

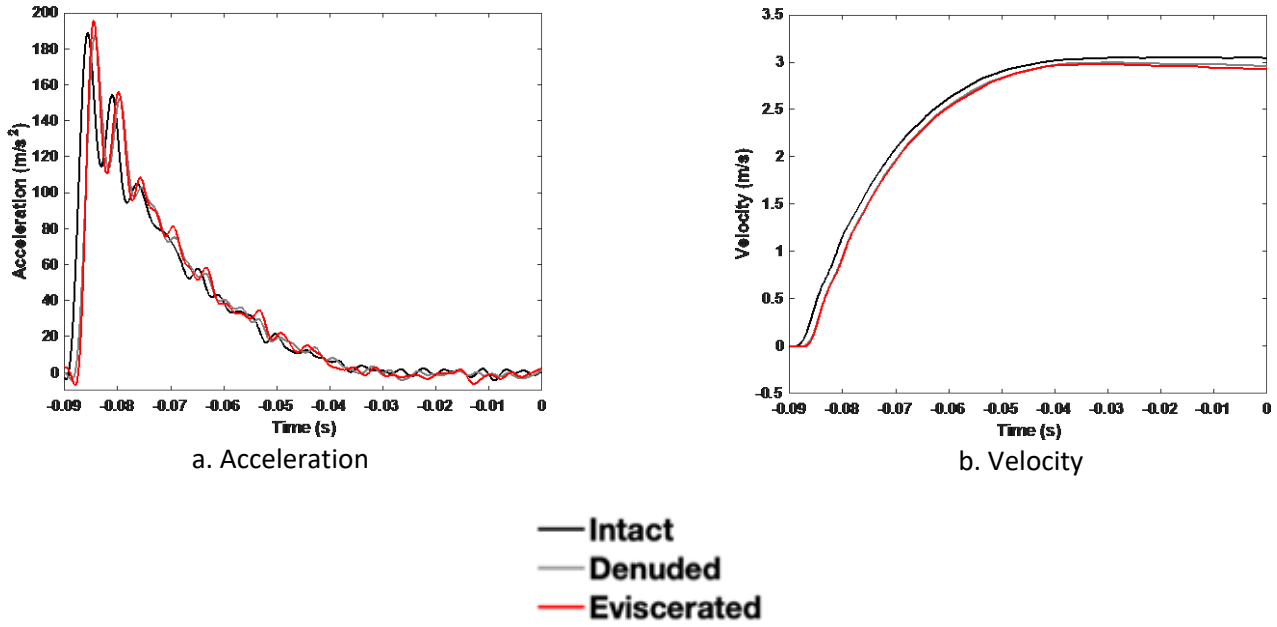

a. Acceleration b. Velocity

Fig. A1. Acceleration curves (a) and calculated velocity curves (b) from the impactor for PMHS A in all three tissue states: intact (black), denuded (gray), and eviscerated (red). Velocity curves (b) show impact speed at 3 m/s just prior to impact at time zero.

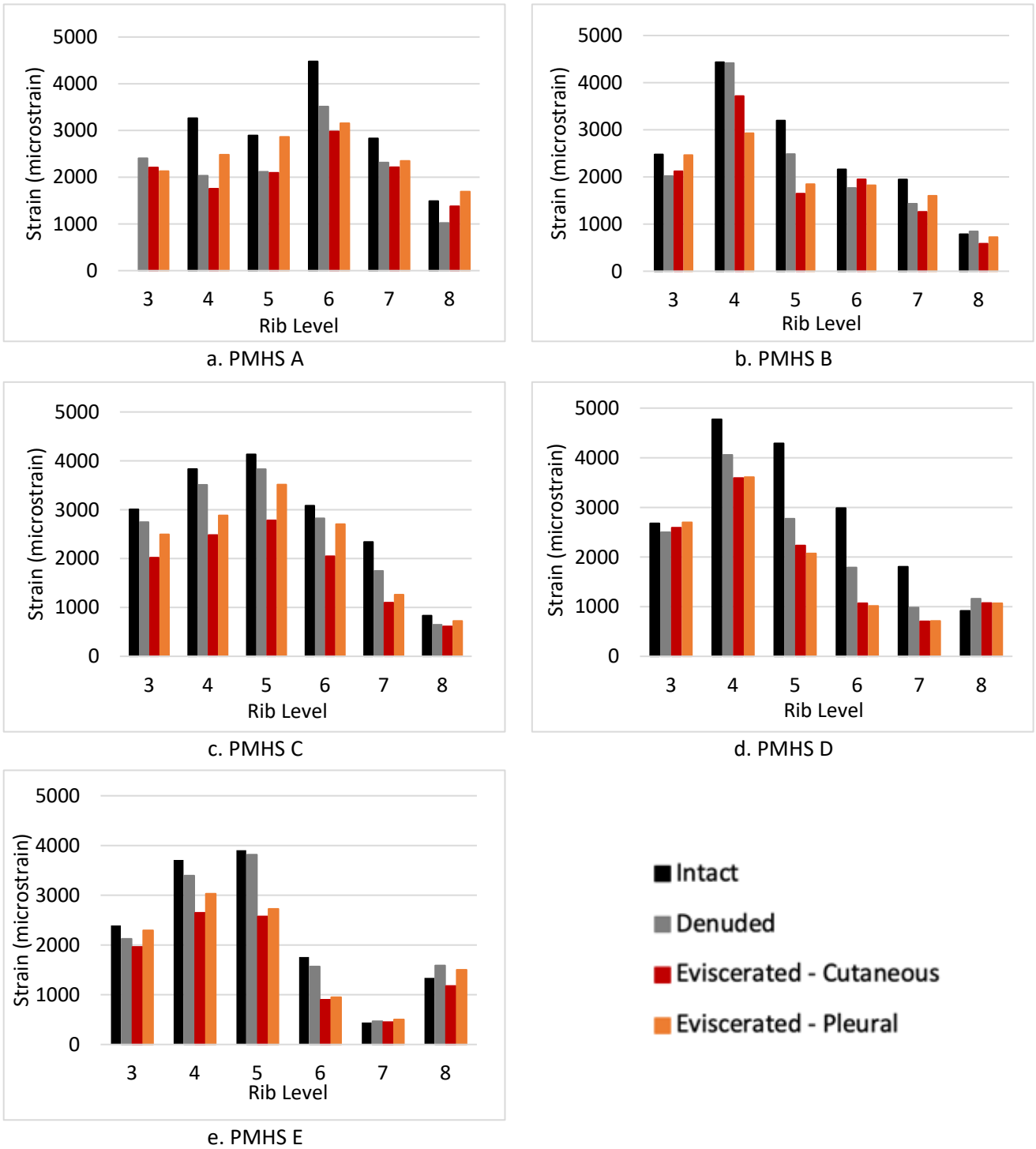

Fig. A2. Absolute peak strain presented as averages of left and right sides by rib level for PMHS A-E in intact, denuded and eviscerated tissue states from the cutaneous surface gauges. Orange bars represent pleural surface gauges from the eviscerated tests. All gauges are from the anterior location.

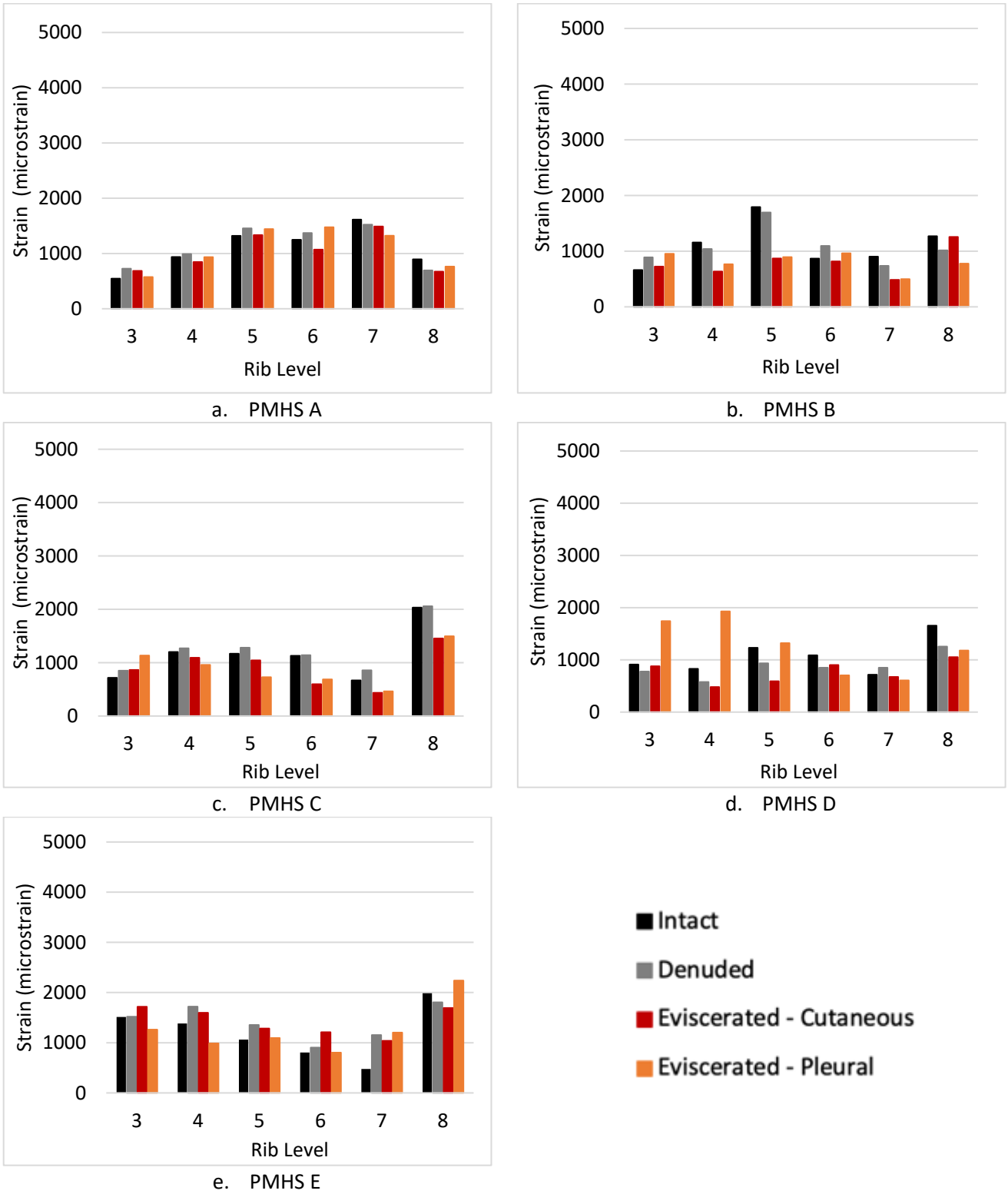

Fig. A3. Absolute peak strain by rib level for PMHS A-E in intact, denuded and eviscerated tissue states from the cutaneous surface gauges. Orange bars represent pleural surface gauges from the eviscerated tests. All gauges are from the posterior location.

TABLE AI

ABSOLUTE PEAK STRAIN (MICROSTRAIN) AT ANTERIOR LOCATIONS FOR ALL SUBJECTS

	Level	PMHS A		PMHS B		PMHS C		PMHS D		PMHS E		Avg. ± St.Dev.
		R	L	R	L	R	L	R	L	R	L	
Intact	3	-	-	3194	1758	2939	3074	2162	3196	3083	1703	2639 ± 652
	4	5795	729	4956	3911	4423	3243	5056	4489	3985	3432	4002 ± 1385
	5	4275	1509	3922	2468	4110	4154	4498	4082	4891	2917	3683 ± 1048
	6	4429	4526	1456	2864	3112	3053	2895	3075	2006	1513	2893 ± 1049
	7	3791	1868	2207	1686	2279	2399	1969	1642	398	486	1872 ± 968
	8	2039	940	811*	758*	1099*	564*	794*	1040*	1283*	1394*	1072 ± 422
	Level	PMHS A		PMHS B		PMHS C		PMHS D		PMHS E		Avg. ± St.Dev.
		R	L	R	L	R	L	R	L	R	L	
Denuded	3	2090	2720	2994	1045	2512	2980	2113	2886	2689	1559	2359 ± 652
	4	3536	528	5067	3761	3585	3432	4129	3989	3441	3349	3482 ± 1156
	5	3191	1043	4105	865	3240	4420	2925	2618	4587	3045	3004 ± 1265
	6	3285	3740	1111	2421	2601	3047	2100	1479	1750	1385	2292 ± 880
	7	2908	1719	1858	1006	1598	1896	979	984	664	271	1388 ± 760
	8	1407*	636*	766*	924*	616*	675*	1238*	1084*	1655*	1521*	1052 ± 387
	Level	PMHS A		PMHS B		PMHS C		PMHS D		PMHS E		Avg. ± St.Dev.
		R	L	R	L	R	L	R	L	R	L	
Eviscerated (Cutaneous)	3	1779	2637	2551	1692	1852	2184	2462	2720	2462	1460	2180 ± 450
	4	2881	629	3486	3944	2514	2448	3424	3761	2520	2776	2838 ± 948
	5	3046	1143	2027	1265	2243	3322	2254	2213	2941	2207	2266 ± 708
	6	2688	3269	750	3147	1934	2161	1273	864	1006	792	1788 ± 989
	7	2792	1636	846	1675	1206	989	736	674	498	404	1146 ± 723
	8	1950*	807*	578*	592*	522*	702*	866*	1283*	1149*	1206*	966 ± 441
	Level	PMHS A		PMHS B		PMHS C		PMHS D		PMHS E		Avg. ± St.Dev.
		R	L	R	L	R	L	R	L	R	L	
Eviscerated (Pleural)	3	2346*	1916*	2304*	2622*	2448*	2544*	2675*	2720*	2221*	2367*	2416 ± 242
	4	2606*	2356*	3012*	2842*	2951*	2814*	3459*	3761*	2659*	3401*	2986 ± 434
	5	3415*	2308*	1847*	-	3183*	3844*	1930*	2213*	2723*	2730*	2604 ± 686
	6	3490*	2819*	699*	2946*	2414*	2996*	1165*	864*	1021*	879*	1929 ± 1095
	7	2733*	1966*	1312*	1885*	1613*	909*	751	674	562	444	1285 ± 750
	8	2505*	881*	611	835	861	584	856	1283	1367	1636	1142 ± 586

*Denotes compression strain mode

R = right rib and L = left rib

TABLE AII

ABSOLUTE PEAK STRAIN (MICROSTRAIN) AT POSTERIOR LOCATIONS FOR ALL SUBJECTS

	Level	PMHS A		PMHS B		PMHS C		PMHS D		PMHS E		Avg. ± St.Dev.
		R	L	R	L	R	L	R	L	R	L	
Intact	3	416	675	771	553	721	714	804	1018	1764	1261	870 ± 391
	4	521	1354	787	1526	1446	954	975	682	1502	1265	1101 ± 365
	5	1115	1525	1809	1774	1176	1159	1520	943	1143	981	1315 ± 317
	6	1761	737	628	1103	1094	1164	1244	931	944	665	1027 ± 334
	7	2163	1065	615*	1187*	787*	549*	654*	776*	-	954*	875 ± 494
	8	858*	931*	925*	1612*	1761*	2304*	1850*	1462*	1778*	2193*	1567 ± 520

	Level	PMHS A		PMHS B		PMHS C		PMHS D		PMHS E		Avg. ± St.Dev.
		R	L	R	L	R	L	R	L	R	L	
Denuded	3	704	747	1325	454	510	1189	427	1129	1586	1449	952 ± 435
	4	1014	965	1086	993	1208	1332	482	671	1823	1614	1119 ± 402
	5	1065	1846	2025	1364	1021	1542	899	970	1420	1286	1344 ± 378
	6	1505	1236	1227	959	1244	1037	794	904	933	876	1071 ± 223
	7	1692	1353	659*	815*	1075*	638*	460*	1242*	1352*	954*	1024 ± 389
	8	432*	958*	803*	1224*	2182*	1933*	1080*	1429*	1529*	2083*	1365 ± 576

	Level	PMHS A		PMHS B		PMHS C		PMHS D		PMHS E		Avg. ± St.Dev.
		R	L	R	L	R	L	R	L	R	L	
Eviscerated (Cutaneous)	3	721	647	810	636	693	1035	433	1322	2019	1416	973 ± 483
	4	1009	682	615	655	1047	1137	554	405	1640	1553	930 ± 423
	5	1171	1497	949	787	882	1203	522	660	1348	1220	1024 ± 314
	6	1383	759	911	721	544	649	789	1014	1588	831	919 ± 329
	7	1520	1458	493	477	443	427	366*	981*	1169*	909*	824 ± 445
	8	753*	593*	1556*	953*	1695*	1213*	820*	1285*	1445*	1939*	1225 ± 441

	Level	PMHS A		PMHS B		PMHS C		PMHS D		PMHS E		Avg. ± St.Dev.
		R	L	R	L	R	L	R	L	R	L	
Eviscerated (Pleural)	3	615*	532*	1127*	778*	1072*	1198*	470*	3014*	889*	1634*	1133 ± 749
	4	1204*	664*	842*	688*	870*	1048*	393*	3462*	1318*	654*	1114 ± 870
	5	1761*	1123*	768*	1018*	768*	686*	635*	2005*	994*	1196*	1095 ± 458
	6	1450*	1501*	874*	1047*	652*	720*	658*	752*	824*	781*	926 ± 312
	7	1527*	1118*	498*	-	471*	455*	498	715	1202	-	818 ± 415
	8	922	603	686	864	1632	1358	1035	1324	1903	2577	1290 ± 612

*Denotes compression strain mode

R = right rib and L = left rib

TABLE AIII

ANTERIOR-POSTERIOR CHEST DEPTHS AND PEAK THORAX COMPRESSION FOR ALL SUBJECTS

		PMHS A	PMHS B	PMHS C	PMHS D	PMHS E
Intact	Chest Depth (mm)	230	250	205	225	200
	Peak Compression (%)	19.3	19.4	18.9	19.5	17.6
		PMHS A	PMHS B	PMHS C	PMHS D	PMHS E
Denuded	Chest Depth (mm)	220	225	200	215	200
	Peak Compression (%)	17.3	18.7	18.0	18.9	17.3
		PMHS A	PMHS B	PMHS C	PMHS D	PMHS E
Eviscerated	Chest Depth (mm)	225	235	210	225	200
	Peak Compression (%)	19.1	19.7	18.6	18.1	18.5

TABLE AIV

DESCRIPTIVE STATISTICS FOR ANTERIOR AND POSTERIOR CUTANEOUS PEAK STRAIN BY RIB LEVEL

	Rib Level	N	Mean ± Std. Dev	95% CI Lower Bound	95% CI Upper Bound	Minimum	Maximum
Anterior Peak Strain (microstrain)	3	*28	2375 ± 595	2026	2723	1045	3196
	4	30	3441 ± 1234	3104	3777	528	5795
	5	30	2984 ± 1157	2647	3321	865	4891
	6	30	2324 ± 1047	1988	2661	750	4526
	7	30	1469 ± 852	1132	1806	271	3791
	8	30	1030 ± 405	693	1367	522	2038
Posterior Peak Strain (microstrain)	3	30	932 ± 425	784	1079	416	2019
	4	30	1050 ± 393	902	1198	405	1823
	5	30	1228 ± 357	1080	1375	522	2025
	6	30	1006 ± 297	858	1153	544	1760
	7	30	939 ± 436	789	1089	366	2163
	8	30	1386 ± 518	1238	1533	431	2304

*Strain data collected were not reliable and were removed from the analysis

TABLE AV

ABSOLUTE PEAK STRAIN RATE (STRAIN/S) AT ANTERIOR LOCATIONS FOR ALL SUBJECTS

	Level	PMHS A		PMHS B		PMHS C		PMHS D		PMHS E		Avg. ± St.Dev.
		R	L	R	L	R	L	R	L	R	L	
Intact	3	-	-	0.337	0.305	0.428	0.368	0.318	0.376	0.447	0.245	0.353 ± 0.066
	4	0.721	0.154	0.408	0.475	0.478	0.357	0.576	0.500	0.538	0.377	0.458 ± 0.150
	5	0.576	0.200	0.394	1.047	0.457	0.371	0.355	0.355	0.560	0.359	0.467 ± 0.231
	6	0.409	0.485	0.205	0.299	0.363	0.312	0.233	0.280	0.300	0.222	0.311 ± 0.088
	7	0.288	0.226	0.250	0.279	0.321	0.283	0.289	0.217	0.103	0.121	0.238 ± 0.073
	8	0.277	0.189	0.164	0.162	0.145	0.139	0.146	0.135	0.185	0.175	0.172 ± 0.042
	Level	PMHS A		PMHS B		PMHS C		PMHS D		PMHS E		Avg. ± St.Dev.
		R	L	R	L	R	L	R	L	R	L	
Denuded	3	0.499	0.669	0.442	0.225	0.382	0.404	0.366	0.477	0.409	0.321	0.419 ± 0.118
	4	0.822	0.146	0.806	0.539	0.575	0.547	0.523	0.594	0.588	0.609	0.575 ± 0.184
	5	1.050	0.264	0.728	0.383	0.648	0.554	0.576	0.635	0.584	0.448	0.587 ± 0.213
	6	0.642	0.462	0.422	0.384	0.515	0.422	0.344	0.302	0.237	0.199	0.393 ± 0.132
	7	0.430	0.276	0.320	0.372	0.410	0.357	0.207	0.241	0.240	0.157	0.301 ± 0.091
	8	0.387	0.244	0.149	0.212	0.194	0.168	0.169	0.137	0.221	0.246	0.213 ± 0.072
	Level	PMHS A		PMHS B		PMHS C		PMHS D		PMHS E		Avg. ± St.Dev.
		R	L	R	L	R	L	R	L	R	L	
Eviscerated (Cutaneous)	3	0.536	0.621	0.360	0.349	0.320	0.265	0.594	0.391	0.513	0.371	0.432 ± 0.123
	4	0.627	0.195	0.447	0.563	0.370	0.439	0.570	0.758	0.429	0.704	0.510 ± 0.168
	5	1.023	0.364	0.278	0.269	0.399	0.737	0.479	0.438	0.587	0.395	0.497 ± 0.232
	6	0.632	0.594	0.326	0.492	0.385	0.357	0.310	0.186	0.132	0.143	0.356 ± 0.176
	7	0.503	0.182	0.260	0.305	0.213	0.210	0.170	0.201	0.315	0.160	0.252 ± 0.103
	8	0.387	0.221	0.129	0.183	0.174	0.143	0.144	0.152	0.589	0.299	0.242 ± 0.147
	Level	PMHS A		PMHS B		PMHS C		PMHS D		PMHS E		Avg. ± St.Dev.
		R	L	R	L	R	L	R	L	R	L	
Eviscerated (Pleural)	3	0.629	0.454	0.345	0.561	0.356	0.283	0.553	0.441	0.488	0.527	0.464 ± 0.110
	4	0.557	0.686	0.409	0.449	0.411	0.516	0.629	0.641	0.466	0.960	0.572 ± 0.168
	5	0.964	0.629	0.267	-	0.581	0.836	0.448	0.394	0.539	0.511	0.574 ± 0.215
	6	0.762	0.556	0.339	0.455	0.515	0.478	0.317	0.209	0.139	0.148	0.392 ± 0.199
	7	0.421	0.211	0.312	0.365	0.230	0.204	0.168	0.219	0.260	0.190	0.258 ± 0.082
	8	0.358	0.283	0.205	0.276	0.178	0.150	0.157	0.161	0.395	0.393	0.255 ± 0.099

TABLE AVI

ABSOLUTE PEAK STRAIN RATE (STRAIN/S) AT POSTERIOR LOCATIONS FOR ALL SUBJECTS FROM THORAX TESTS

	Level	PMHS A		PMHS B		PMHS C		PMHS D		PMHS E		Avg. ± St.Dev.
		R	L	R	L	R	L	R	L	R	L	
Intact	3	0.185	0.187	0.102	0.102	0.151	0.144	0.139	0.119	0.236	0.196	0.156 ± 0.044
	4	0.178	0.346	0.199	0.199	0.204	0.216	0.200	0.159	0.183	0.117	0.200 ± 0.059
	5	0.298	0.244	0.265	0.265	0.311	0.287	0.396	0.193	0.142	0.146	0.255 ± 0.078
	6	0.144	0.184	0.165	0.165	0.260	0.270	0.181	0.222	0.109	0.076	0.178 ± 0.061
	7	0.217	0.161	0.156	0.156	0.137	0.129	0.153	0.162	-	0.087	0.151 ± 0.034
	8	0.161	0.086	0.100	0.100	0.157	0.180	0.150	0.119	0.164	0.224	0.144 ± 0.043
	Level	PMHS A		PMHS B		PMHS C		PMHS D		PMHS E		Avg. ± St.Dev.
		R	L	R	L	R	L	R	L	R	L	
Denuded	3	0.238	0.229	0.211	0.167	0.120	0.120	0.141	0.184	0.218	0.300	0.193 ± 0.058
	4	0.526	0.444	0.464	0.193	0.287	0.287	0.217	0.296	0.415	0.403	0.353 ± 0.112
	5	0.496	0.303	0.370	0.299	0.267	0.267	0.355	0.355	0.273	0.225	0.321 ± 0.077
	6	0.271	0.215	0.279	0.210	0.273	0.273	0.308	0.256	0.209	0.155	0.245 ± 0.046
	7	0.340	0.335	0.210	0.218	0.251	0.251	0.106	0.232	0.224	0.149	0.232 ± 0.072
	8	0.140	0.198	0.134	0.140	0.304	0.304	0.187	0.195	0.182	0.236	0.202 ± 0.062
	Level	PMHS A		PMHS B		PMHS C		PMHS D		PMHS E		Avg. ± St.Dev.
		R	L	R	L	R	L	R	L	R	L	
Eviscerated (Cutaneous)	3	0.267	0.148	0.175	0.105	0.123	0.197	0.255	0.253	0.236	0.401	0.216 ± 0.087
	4	0.457	0.215	0.237	0.212	0.245	0.322	0.196	0.314	0.183	0.396	0.278 ± 0.092
	5	0.591	0.251	0.204	0.286	0.217	0.334	0.300	0.228	0.142	0.312	0.286 ± 0.121
	6	0.361	0.240	0.308	0.194	0.298	0.337	0.359	0.276	0.109	0.302	0.278 ± 0.079
	7	0.319	0.262	0.176	0.164	0.170	0.173	0.123	0.288	-	0.219	0.211 ± 0.066
	8	0.140	0.187	0.211	0.169	0.261	0.170	0.082	0.157	0.164	0.283	0.182 ± 0.058
	Level	PMHS A		PMHS B		PMHS C		PMHS D		PMHS E		Avg. ± St.Dev.
		R	L	R	L	R	L	R	L	R	L	
Eviscerated (Pleural)	3	0.316	0.238	0.224	0.178	0.251	0.242	0.294	0.254	0.410	0.544	0.295 ± 0.107
	4	0.528	0.288	0.253	0.192	0.287	0.337	0.152	0.533	0.434	0.172	0.318 ± 0.140
	5	0.687	0.282	0.154	0.375	0.288	0.296	0.313	0.310	0.318	0.366	0.339 ± 0.136
	6	0.483	0.255	0.307	0.230	0.316	0.383	0.330	0.230	0.164	0.181	0.288 ± 0.097
	7	0.324	0.220	0.198	-	0.151	0.190	0.245	0.241	0.205	-	0.222 ± 0.051
	8	0.154	0.220	0.115	0.161	0.239	0.200	0.148	0.179	0.365	0.301	0.208 ± 0.077

TABLE AVII

DESCRIPTIVE STATISTICS FOR ANTERIOR AND POSTERIOR CUTANEOUS PEAK STRAIN RATE BY RIB LEVEL

	Rib Level	N	Mean ± Std. Dev	95% CI Lower Bound	95% CI Upper Bound	Minimum	Maximum
Anterior Peak Strain Rate (strain/s)	3	*28	0.405 ± 0.109	0.350	0.459	0.225	0.669
	4	30	0.514 ± 0.169	0.462	0.567	0.146	0.822
	5	30	0.517 ± 0.223	0.464	0.570	0.200	0.851
	6	30	0.353 ± 0.136	0.301	0.406	0.132	0.642
	7	30	0.263 ± 0.091	0.211	0.316	0.103	0.503
	8	30	0.209 ± 0.098	0.156	0.261	0.129	0.589
Posterior Peak Strain Rate (strain/s)	3	30	0.188 ± 0.068	0.159	0.217	0.102	0.401
	4	30	0.277 ± 0.108	0.248	0.306	0.198	0.526
	5	30	0.290 ± 0.095	0.258	0.316	0.227	0.591
	6	30	0.234 ± 0.075	0.205	0.263	0.177	0.361
	7	*28	0.200 ± 0.067	0.169	0.229	0.154	0.340
	8	30	0.176 ± 0.058	0.147	0.205	0.140	0.304

*Strain data collected were not reliable and were removed from the analysis

TABLE AVIII

ABSOLUTE PEAK STRAIN (MICROSTRAIN) OF ANTERIOR AND POSTERIOR LOCATIONS FROM INDIVIDUAL RIB TESTING

	Level	PMHS A		PMHS B		PMHS C		PMHS D		PMHS E		Avg ± St.Dev.
		R	L	R	L	R	L	R	L	R	L	
Anterior Cutaneous	4	6533	7695	5858	4641	13255	8820	6552	6911	10185	11132	8158 ± 2667
	5	7179	1166	9217	6812	16404	12641	9202	6667	16040	12924	9825 ± 4728
	6	7671	15972	8073	7733	16317	9659	7905	5465	12526	13669	10499 ± 3834
	7	11278	-	8621	7929	23103	16100	9114	6885	15791	14111	12548 ± 5235
	Level	PMHS A		PMHS B		PMHS C		PMHS D		PMHS E		Avg ± St.Dev.
		R	L	R	L	R	L	R	L	R	L	
**Anterior Pleural*	4	9433	6347	2745	4074	10980	7669	7025	6255	8104	11428	7406 ± 2769
	5	7561	6584	7560	6175	14114	11868	7609	6858	10738	8860	8793 ± 2614
	6	8695	13750	6863	6964	14127	14358	7804	6142	5383	11228	9531 ± 3515
	7	9802	11279	7083	10736	20250	26701	9807	6358	11905	11305	12523 ± 6234
	Level	PMHS A		PMHS B		PMHS C		PMHS D		PMHS E		Avg ± St.Dev.
		R	L	R	L	R	L	R	L	R	L	
Posterior Cutaneous	4	11808	9583	5662	5197	16662	9348	3611	5917	11778	11108	9068 ± 3990
	5	9545	8614	8614	5847	20608	8130	8694	7305	18400	9530	10529 ± 4879
	6	9672	13407	7527	7172	21187	15923	8367	6649	10210	10800	11091 ± 4579
	7	11126	17173	6341	6322	14748	22407	5112	7666	8663	8607	10817 ± 5603
	Level	PMHS A		PMHS B		PMHS C		PMHS D		PMHS E		Avg ± St.Dev.
		R	L	R	L	R	L	R	L	R	L	
**Posterior Pleural*	4	11101	11768	3665	5842	10866	9659	2837	7770	10720	-	8248 ± 3387
	5	11041	8391	6613	8442	14227	7239	7397	7719	10665	6273	8801 ± 2472
	6	10944	10574	6712	8340	22518	14670	10159	5958	10147	4817	10484 ± 5101
	7	15340	12476	6435	8100	10593	22749	9248	6566	7316	13268	11209 ± 5050

*Denotes pleural gauges in compression

R= right rib and L = left rib

TABLE AIX

DESCRIPTIVE STATISTICS FOR ANTERIOR AND POSTERIOR CUTANEOUS PEAK STRAIN BY RIB LEVEL FROM INDIVIDUAL RIB TESTS

	Rib Level	N	Mean ± Std. Dev	95% CI Lower Bound	95% CI Upper Bound	Minimum	Maximum
Anterior Peak Strain (microstrain)	4	10	8158 ± 2667	5463	10853	4641	13255
	5	10	9825 ± 4729	7130	12520	1166	16404
	6	10	10499 ± 3834	7804	3834	5465	16317
	7	*9	12548 ± 5235	9707	15389	6885	23103
Posterior Peak Strain (microstrain)	4	10	9067 ± 3991	5990	12145	3611	16662
	5	10	10529 ± 4879	7451	13606	5847	20608
	6	10	11091 ± 4579	8014	14169	6649	21187
	7	10	10817 ± 5603	7739	13894	5112	22407

*Strain data collected were not reliable and was removed from analysis